

Slip-draft embedded control system by adaptively adjusting the battery position for electric tractor

Minghui Wang¹, Pucal Ning², Ke Su³, Gejima Yoshinori⁴,
Wei Wang¹, Yongjie Cui^{1,5,6*}, Gongpei Cui^{7*}

(1. College of Mechanical and Electronic Engineering, Northwest A & F University, Yangling 712100, Shaanxi, China;

2. SAIC Motor Technical Center, Shanghai 201804, China;

3. School of Arts and Design, Qilu University of Technology (Shandong Academy of Sciences), Jinan 250353, China;

4. Faculty of Agriculture, University of Miyazaki, Miyazaki 8892192, Japan;

5. Key Laboratory of Agricultural Internet of Things, Ministry of Agriculture and Rural Affairs, Yangling 712100, Shaanxi, China;

6. Shaanxi Key Laboratory of Agricultural Information Perception and Intelligent Service, Yangling 712100, Shaanxi, China;

7. College of Mechanical & Electrical Engineering, Henan Agricultural University, Zhengzhou 450002, China)

Abstract: A slip-draft embedded control system was designed and developed for an independent developed 2WD (two-wheel drive) electric tractor, to improve the traction efficiency, operation performance and ploughing depth stability of the electric tractor. In this system, the battery of electric tractor was innovatively equivalent to the original counterweight of the fuel tractor. And through dynamic analysis of electric tractor during ploughing, the mathematical model of adjusting the center of gravity about draft force and slip rate was established. Then the automatic adjustment of the center of gravity for electric tractor was realized through the adaptive adjustment of battery position. Finally, the system was carried on electric tractor for performance evaluation under different ploughing conditions, the traction efficiency, slip rate and front wheel load of electric tractor were measured and controlled synchronously to make it close to the set range. And the comparative experiments of ploughing operation were carried out under the two modes of adaptive adjustment of center of gravity and fixed center of gravity. The test results showed that, based on the developed control system, the center of gravity of electric tractor can be adjusted in real time according to the complex changes of working conditions. During ploughing operation with adjusting adaptively battery position, the average values of traction efficiency, slip rate, front wheel load and relative error of tillage depth of electric tractor were 64.5%, 22.2%, 2045.0 N and 2.0% respectively. Which were optimized by 15.0%, 29.5%, 19.6% and 80.0% respectively, compared with electric tractor with fixed battery position. The slip-draft embedded control system can not only realize the adaptive adjustment of the center of gravity position in the ploughing process of electric tractor, but also improve the traction efficiency and the stability of ploughing depth, which can provide reference for the actual production operation of electric tractor.

Keywords: electric tractor, embedded control system, adjusting adaptively, center of gravity position, performance test

DOI: 10.25165/ijabe.20231605.7280

Citation: Wang M H, Ning P C, Su K, Yoshinori G, Wang W, Cui Y J, et al. Slip-draft embedded control system by adaptively adjusting the battery position for electric tractor. *Int J Agric & Biol Eng*, 2023; 16(5): 155–164.

1 Introduction

With the intensification of global energy crisis and environmental pollution, the electrification of agricultural machinery aiming at carbon neutralization has become an inevitable trend^[1,2]. Electric tractor has made rapid development, because of

compact structure, simple operation, low carbon, high efficiency and low maintenance cost^[3,4]. Under different operating conditions, the operation stability and traction performance of electric tractor can be effectively improved by changing the weight of counterweight^[5-7]. However, the counterweight of electric tractors is mostly fixed weight or no counterweight at present, which seriously affects its operating performance^[8,9]. Therefore, realizing the automatic, accurate and real-time adjustment of the center of gravity of electric tractor has become an urgent problem, to improve the operation stability and traction performance.

In recent years, the research on adjusting the center of gravity of tractor mainly focuses on the counterweight^[10,11], adjustment device^[12-14] and adjustment method^[15,16], and there is less research on the automatic, accurate and real-time adjustment system for the center of gravity of electric tractor. Janulevicius et al.^[10] determined the weight of the counterweight when the slip rate was in the optimal range through experiments, which provided a reference for improving the tractor's traction performance. Vidas^[17] designed a telescopic front counterweight adjustment mechanism, to realize the adjustment of the tractor's center of gravity by manually adjusting

Received date: 2021-12-16 **Accepted date:** 2023-06-04

Biographies: Minghui Wang, MS, research interest: intelligent agricultural equipment, Email: wangminghui@nwfufu.edu.cn; Pucal Ning, MS, research interest: facility agricultural machinery, Email: ningpucal@163.com; Ke Su, PhD, Associate Professor, research interest: product innovation methods, Email: coco_su0716@163.com; Gejima Yoshinori, PhD, Associate Professor, research interest: agriculture robot, Email: ygejima@cc.miyazaki-u.ac.jp; Wei Wang, PhD, Associate Professor, research interest: power machinery, Email: wangwei79912@nwsuaf.edu.cn.

***Corresponding author:** Yongjie Cui, PhD, Professor, research interest: intelligent agricultural robot. College of Mechanical and Electronic Engineering, Northwest A&F University, Yangling 712100, Shaanxi, China. Tel: +86-13720581232, Email: cuiyongjie@nwsuaf.edu.cn; Gongpei Cui, PhD, Lecturer, research interest: agricultural automation equipment. College of Mechanical & Electrical Engineering, Henan Agricultural University, Zhengzhou 450002, China. Tel: +86-15837181219, Email: cuiyongpei689@163.com.

the longitudinal position of the counterweight. Pranav and Pandey^[18] developed a tractor axle load calculation system based on Visual Basic, by collecting data such as soil, tires and agricultural machinery during tractor operation, which can be used to optimize the tractor counterweight scheme. Liu et al.^[19] proposed a tractor counterweight optimization matching method based on NSGA-II algorithm, and a tractor dynamics model during ploughing operation was established, using NSGA-II algorithm to solve the objective function. Xu et al.^[20] optimized the position of the center of gravity of the power battery box model and the driving space module by using a modular design method, which can ensure that the tractor has the best performance of center of gravity configuration in the pure driving state.

To solve the above problems, the battery of electric tractor was creatively equivalent to the counterweight in this paper, and a slip-draft embedded control system by adjusting adaptively battery position for electric tractor was developed. Firstly, the relationship model between draft force, slip rate and the center of gravity position of electric tractor was established; Secondly, the slip-draft embedded control system and operation parameter measurement unit were selected and designed; Then, the integrated trial production of the embedded control system for electric tractor was carried out; Finally, the adaptability test and performance comparison test of the electric tractor with slip-draft embedded control system during ploughing operation were carried out. The slip-draft embedded control system of electric tractor can provide reference for the improvement of actual production performance of electric tractor.

2 Materials and methods

2.1 Center of gravity adaptive adjustment device

A 2WD electric tractor (Figure 1) was designed and developed based on the chassis of fuel tractor, to carry out the center of gravity adaptive adjustment test. And the electric tractor was composed of tractor chassis, power battery, drive motor, drive motor controller, battery position adjustment mechanism. The height of the center of gravity of electric tractor and the distance from chassis center of gravity to rear axle were measured, and the values were 0.481 m and 0.425 m, respectively. And the main structural performance parameters of electric tractor were tested (Table 1), which showed that the electric tractor basically met the performance indexes of the original fuel tractor.

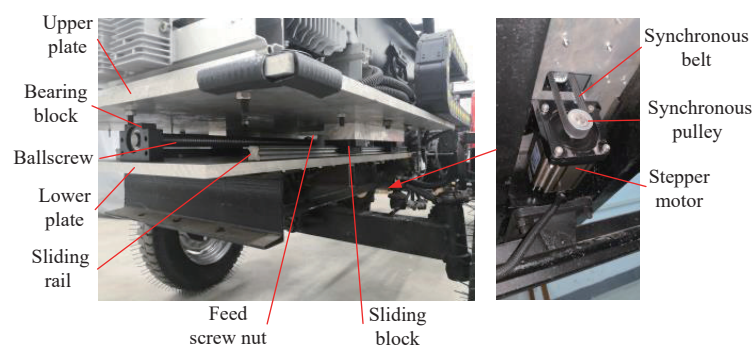


Figure 2 Battery position adjustment mechanism

2.2 Operation parameter measurement unit

The best position of the center of gravity for electric tractor was calculated, according to the slip rate and the draft force. And the position of the power battery was adjusted adaptively with the adaptive adjustment embedded control system. Meanwhile, the operating parameter measurement unit mainly included front wheel

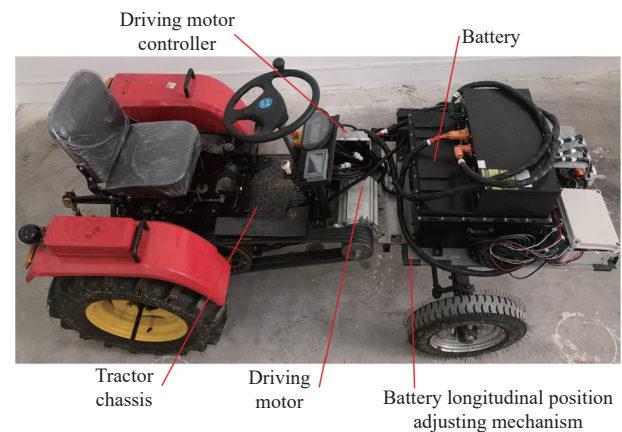


Figure 1 2WD electric tractor

Table 1 Structural performance parameters of electric tractor

Specification	Electric tractor	Original fuel tractor ^[21]
Rated power/kW	10	11
Total weight of the electric tractor/kg	767	760
Wheelbase/m	1.450	1.45
The diameter of front tire/m	0.508	0.508
The diameter of rear tire/m	0.787	0.787
Maximum speed/km·h ⁻¹	21.6	21.0
Maximum draft force/N	4020	3138

The battery position adjustment mechanism (Figure 2) consisted of the upper plate, bearing seat, ball screw, bottom plate, slide, screw nut, slider, stepper motor, pulley and synchronous belt. Where the movable range (a_L) of the slider on the slide was 0 mm to 400 mm, and the limit point close to the stepper motor was set as the starting point (0 mm) of the adjustment range. The movement speed of the slider was 20 mm/s under the action of the stepper motor. The working principle of the battery position adjustment mechanism was as follows: The stepper motor controller drove the stepper motor according to the driving signal, and the power of the stepping motor was transmitted to the ball screw through the timing belt. The screw nut was installed on the ball screw and moved in the longitudinal direction under the drive of the ball screw. Then the power battery was installed on the lead screw nut through the upper bottom plate. The power battery could be moved in the longitudinal direction to complete the adjustment for the electric tractor's center of gravity.

encode, rear wheel encoder, upper pull rod force sensor and two lower pull rod force sensors (Figure 3).

The force sensors were used to measure the draft force of electric tractor to the plowing implement. Aiming at the disadvantages of high assembly accuracy and single force measuring direction of pin type force sensor, a strain gauge

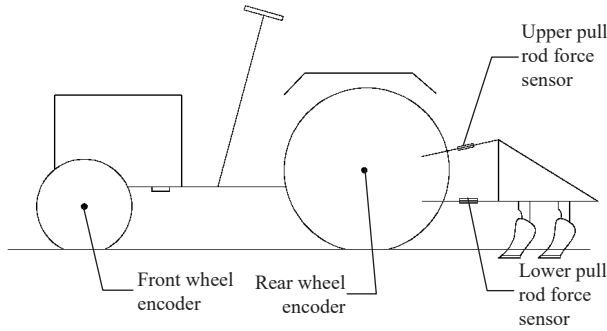


Figure 3 Operation parameter measurement unit

embedded force sensor was designed and manufactured, with the CG/JS-NJ strain gauges embedded in the upper rod and two lower rods respectively. The measuring range of strain gauge embedded force sensor was from -10 kN to 10 kN, and the measuring accuracy was 0.001 N.

The encoders (Omron E6B2-CWZ6C, Shijiazhuang Longge Technology Co., Ltd, China) of the STM32 timer were used to measure the front and rear wheel speed of electric tractor, by

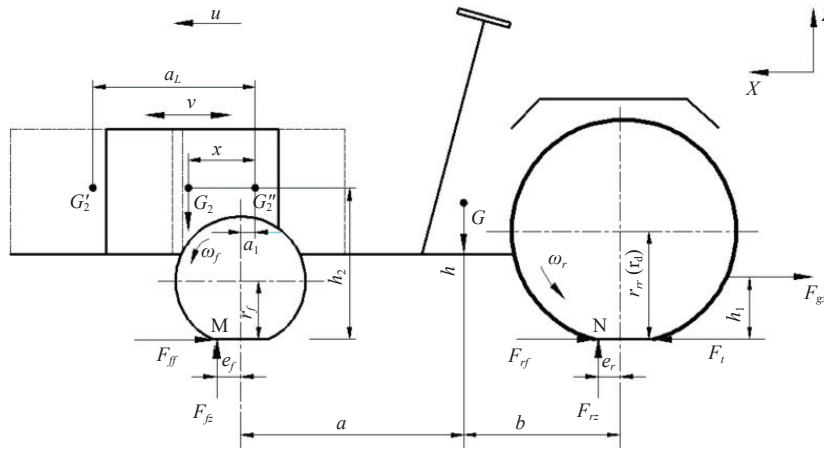


Figure 4 Dynamic analysis of electric tractor during ploughing

During ploughing, the electric tractor ran smoothly and slowly, thus electric tractor was in a state of force balance. The resultant force in vertical direction was expressed in Equation (1).

$$F_{fz} + F_{rz} - G - G_2 = 0 \quad (1)$$

where, F_{fz} is the vertical load on the front wheel, N; F_{rz} is the vertical load on the rear wheel, N; G is the gravity on the tractor chassis, N; G_2 is the gravity on the power battery, N.

The moments of forces at rear wheel (Point N) and front wheel (Point M) were expressed in Equation (2).

$$\begin{cases} N: G_2(x - a_1 + a + b - e_r) + G(b - e_r) - \\ F_{fz}(a + b + e_f - e_r) - F_{gx}h_1 = 0 \\ M: F_{rz}(a + b + e_f - e_r) + G_2(x - a_1 - e_f) - \\ G(a + e_f) - F_{gx}h_1 = 0 \end{cases} \quad (2)$$

where, x is the adjustment distance of battery position, m; a_1 is the distance between the center of gravity of the battery and the front axle (when the battery is in the initial position), m; a is the distance between the front axle and the center of gravity of the chassis, m; b is the distance between the rear wheel and the center of gravity of the chassis, m; e_r is the longitudinal displacement of rear wheel reaction force, m; e_f is the longitudinal displacement of front wheel reaction force, m; F_{gx} is the draft force of electric tractor during ploughing, N; h_1 is the effective height of draft force, m.

collecting the pulse signal and calculating the number of revolutions of the wheel per second, then figure out further the slip rate (Equations (7)-(9)). And the encoders were respectively installed on the left front wheel, left rear wheel and right rear wheel. Among the encoder located on the left front wheel was used to measure the front wheel speed, to obtain further the theoretical speed of the electric tractor. However, there was a differential mechanism on the rear axle of the electric tractor, so the average speed of the two rear wheels obtained by encoders located on the left rear wheel and right rear wheel, was taken as the actual speed of the rear wheels, to obtain further the actual speed of the electric tractor^[18].

2.3 Center of gravity adaptive adjustment control method

2.3.1 Dynamic analysis of electric tractor during ploughing

Dynamic analysis of electric tractor during ploughing was carried out based on the suspension plow with height adjustment (Figure 4). In this suspension plow, the suspension mechanism was only used to transmit the draft force of electric tractor, bearing the weight of the frame and adjusting the tillage depth were realized by the depth-limiting wheel.

In order to ensure the stability of the tractor, the front axle load of the tractor shall not be less than 20% of weight with full equipment^[6,21], so the adjustment distance of battery position was expressed in Equation (3).

$$x = \frac{1}{G_2} [0.2(G + G_2)(a + b + e_f - e_r) - G(b - e_r) + F_{gx}h_1] + a_1 - a - b + e_r \quad (3)$$

The vertical load on the front wheel (F_{fz}) and the vertical load on the rear wheel (F_{rz}) were expressed in Equation (4).

$$\begin{cases} F_{fz} = \frac{1}{(a + b + e_f - e_r)} [G(b - e_r) - F_{gx}h_1 + \\ G_2(x - a_1 + a + b - e_r)] \\ F_{rz} = \frac{1}{(a + b + e_f - e_r)} [G(a + e_f) + F_{gx}h_1 - \\ G_2(x - a_1 - e_f)] \end{cases} \quad (4)$$

As seen in Equation (4), the vertical load on the front wheel decreased with the increase of the draft force. When F_{fz} was less than 20% of the weight with full equipment, the operation stability of the electric tractor would decrease. The adjustment distance of battery position would increase and stay in a certain range by moving the battery position forward, which could increase the front wheel load and maintain a reasonable proportion of the weight with

full equipment. It could effectively improve the driving stability of the electric tractor. Further analysis could be obtained that F_{rz} increased with the increase of F_{gx} . When the slip rate was guaranteed to be within the threshold range, the forward movement of the battery would reduce the vertical load of the rear wheels and improve the traction efficiency.

2.3.2 Calculation method of the draft force

The draft force of the electric tractor was calculated based on the longitudinal projection of the force of the three-point suspension mechanism in the relative position in space (Figure 5). In this study, the height adjustment method was used for ploughing operation, so the vertical force of the machine to the electric tractor could be ignored.

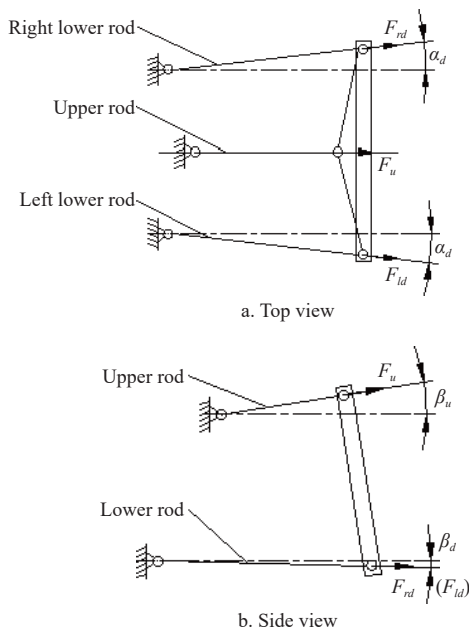


Figure 5 Force relationship of three-point suspension mechanism

The force was balanced during the ploughing operation of the electric tractor. The draft force (F_{gx}) was expressed in Equation (5).

$$F_{gx} = (F_{ld} + F_{rd}) \cos(\alpha_d) \cos(\beta_d) + F_u \cos(\beta_u) \tag{5}$$

where, F_{ld} is the pull force of left lower rod of three-point suspension mechanism, N; F_{rd} is the pull force of right lower rod of three-point suspension mechanism, N; F_u is the pull force of upper rod of three-point suspension mechanism, N; α_d is the angle between the pull force of the lower rod and the vertical direction, ($^\circ$); β_u is the angle between the pull force of the upper rod and the horizontal direction, ($^\circ$); β_d is the angle between the pull force of the lower rod and the horizontal direction, ($^\circ$).

In actual ploughing operation, β_d was a very small value, so the cosine value of β_d was close to 1. The simplified draft force (F_{gx}) was expressed in Equation (6).

$$F_{gx} = (F_{ld} + F_{rd}) \cos(\alpha_d) + F_u \cos(\beta_u) \tag{6}$$

2.3.3 Calculation method of the slip rate

The slip rate of a rear-wheel drive tractor could be calculated based on the speed difference between the front and rear wheels. Where the actual speed of the tractor was calculated by the front wheel speed, and the theoretical speed of the tractor was calculated by the rear wheel speed [5,22].

The actual speed of the tractor was expressed in Equation (7).

$$V_{ac} = \pi r_f \frac{P_{cntf}}{1000t} \tag{7}$$

where, V_{ac} is the actual speed of the tractor, m/s; r_f is the rolling radius of tractor front wheel, m; P_{cntf} is the encoder pulse number of front wheel per unit time; t is the running time, s.

The theoretical speed of the tractor was expressed in Equation (8).

$$\begin{cases} V_{thl} = \pi r_{rl} \frac{P_{cntrl}}{1000t} \\ V_{thr} = \pi r_{rr} \frac{P_{cntrr}}{1000t} \\ V_{th} = \frac{V_{thl} + V_{thr}}{2} \end{cases} \tag{8}$$

where, V_{thl} is the theoretical speed of tractor left rear wheel, m/s; V_{thr} is the theoretical speed of tractor right rear wheel, m/s; V_{th} is the average theoretical tractor speed, m/s; r_{rl} is the rolling radius of tractor left rear wheel, m; r_{rr} is the rolling radius of tractor right rear wheel, m; P_{cntrl} is the encoder pulse number of left rear wheel, s; P_{cntrr} is the encoder pulse number of right rear wheel.

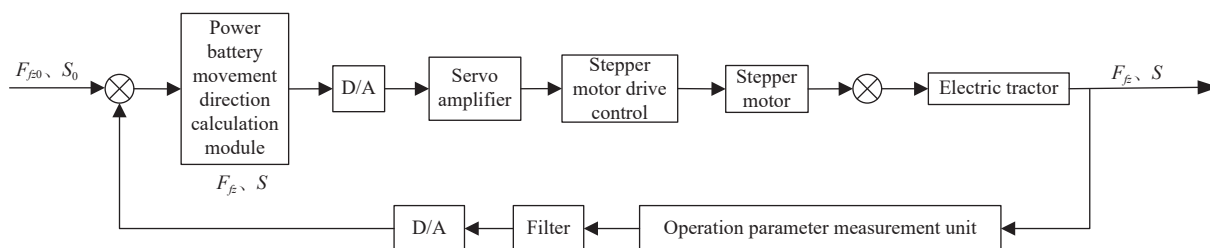
Slip rate of rear wheel was expressed in Equation (9).

$$S = 100 \left(1 - \frac{V_{ac}}{V_{th}} \right) \tag{9}$$

where, S is the slip rate of rear wheel, %.

2.3.4 Slip-draft automatic control method by adjusting adaptively battery position

The slip-draft embedded control system by adjusting adaptively battery position for electric tractor was a closed-loop system (Figure 6). The force sensor signal and the encoder signal were filtered and A/D converted to calculate the actual vertical load on front wheel and slip rate of rear wheel, then the deviation was obtained compared with the set value. And the deviation signal was transmitted to the control unit, and the power battery motion direction was calculated according to the input vertical load of the front wheel and the deviation signal by the power battery motion direction calculation module. The solution signal was transmitted to the stepper motor driver after D/A conversion and servo amplifier amplification. The forward and reverse operation of the stepper motor was controlled by stepper motor driver, according to the input control signal, to make the power battery move in the corresponding direction for adjusting the center of gravity of the electric tractor.



Note: F_{fz0} is the target vertical load on front wheel of electric tractor, N; S_0 is the target slip rate of rear wheel of electric tractor, %; F_{fz} is the actual vertical load on front wheel of electric tractor, N; S is the slip rate of rear wheel of electric tractor, %.

Figure 6 Slip-draft embedded closed-loop control system by adjusting adaptively battery position

As known in Figure 7, when the slip rate exceeded the optimal range, the battery position was adaptively adjusted, according to the relationship between the front wheel load and 20% of the whole machine weight. Namely, when the front wheel load was less than 20% of the whole machine weight, the battery was controlled to move forward. And when the front wheel load was higher than 20% of the whole machine weight, the battery was controlled to move backward. Above control method for adjusting battery position kept the slip rate in the optimal range, maintained the uniform tillage depth and improved the tractor traction efficiency.

2.4 Center of gravity adaptive adjustment control system integration

The center of gravity adaptive adjustment embedded control system included three encoders, three force sensors, stepper motors, stepper motor drivers, STM32 single-chip microcomputers and upper computer software (Figure 8). The data from encoders and force sensors were collected by the single-chip microcomputer with the STM32F103ZET6 chip, then the slip rate of driving wheel and the draft force were calculated. Then the main control unit controlled the rotation of the stepping motor to complete the longitudinal movement of the battery position. At the same time, the data collected and processed by the single-chip microcomputer was transmitted to the upper computer through the Bluetooth module. And the upper computer displayed the parameter values of the electric tractor in real time and stored the data in EXCEL (Figure 9), included the left front wheel speed, the left rear wheel speed, the right rear wheel speed, the left pull-down rod force, the right pull

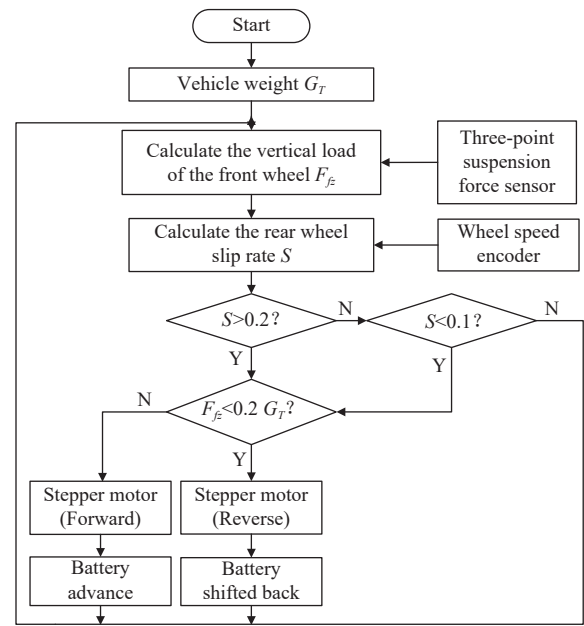


Figure 7 Embedded control method for adjusting adaptively battery position

rod force, the pull rod force, the actual tractor speed, the horizontal draft force of tractor, the vertical resultant force, the location of the battery, the battery adjustment distance, the slip rate of driving wheel, the time of data collection.

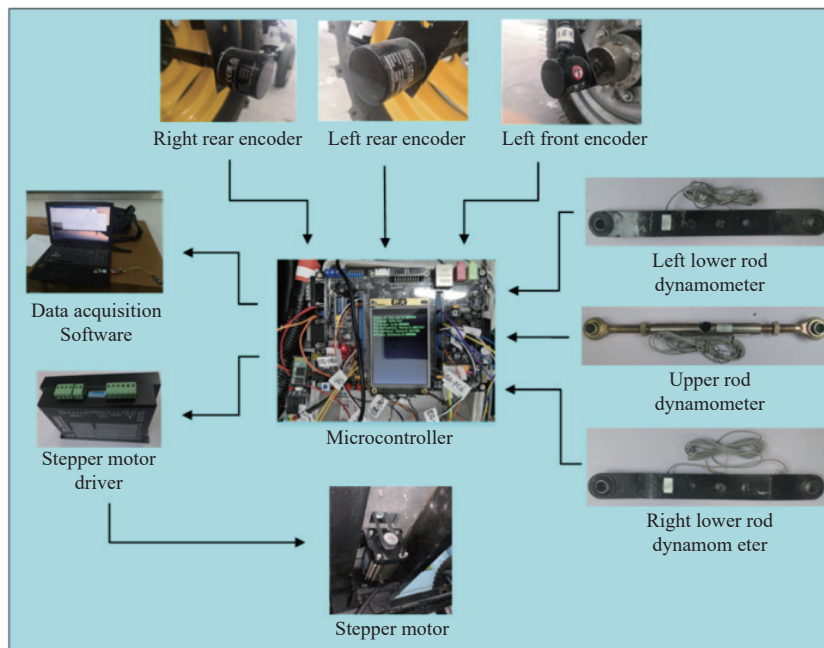


Figure 8 Development process of the center of gravity adaptive adjustment control system

FWRS(r/s)	LRWRS(r/s)	RRWRS(r/s)	LDRF(N)	RDRF(N)	URF(N)	ACS(m/s)	Fgx(N)	Fgz(N)	BP(mm)	BAPx(mm)	S	Acquisition Time
0.0	0.0	0.0	2624.5	2345.0	0.0	0.0	1172.5	938.0	0.0	0.0	0.0	2021-01-10 15:59:01.585668
0.0	0.0	0.0	2624.5	2343.8	0.0	0.0	1171.9	937.5	0.0	0.0	0.0	2021-01-10 15:59:01.503680
0.0	0.0	0.0	2625.8	2343.8	0.0	0.0	1171.9	937.5	0.0	0.0	0.0	2021-01-10 15:59:01.424100
0.0	0.0	0.0	2629.4	2347.4	0.0	0.0	1173.7	938.9	0.0	0.0	0.0	2021-01-10 15:59:01.329402
0.0	0.0	0.0	2624.5	2343.8	0.0	0.0	1171.9	937.5	0.0	0.0	0.0	2021-01-10 15:59:01.245851
0.0	0.0	0.0	2624.5	2345.0	0.0	0.0	1172.5	938.0	0.0	0.0	0.0	2021-01-10 15:59:01.156272
0.0	0.0	0.0	2624.5	2345.0	0.0	0.0	1172.5	938.0	0.0	0.0	0.0	2021-01-10 15:59:01.056573
0.0	0.0	0.0	2627.0	2346.2	0.0	0.0	1173.1	938.5	0.0	0.0	0.0	2021-01-10 15:59:00.964300
0.0	0.0	0.0	2624.5	2345.0	0.0	0.0	1172.5	938.0	0.0	0.0	0.0	2021-01-10 15:59:00.885002
0.0	0.0	0.0	2624.5	2345.0	0.0	0.0	1172.5	938.0	0.0	0.0	0.0	2021-01-10 15:59:00.773583

Figure 9 Display interface of data acquisition

The center of gravity adaptive adjustment embedded control system software was mainly used to complete the functions of system initialization, fault detection and communication interface control (Figure 10). Specifically, the system was initialized firstly to detect whether the communication connection of each device was normal. Secondly, the data was collected from the force sensors and the encoders and loaded into the buffer. Then, the buffer data was read and calculated by the power battery movement direction calculation module. Finally, the motion direction control command of the stepper motor driver was sent to the stepper motor driver. After a control instruction was sent, the system continued to read and calculate the buffer data and update the control instruction. The connection circuit of each component of the center of gravity adaptive adjustment embedded control system is shown in Figure 11. And the hardware and software of the center of gravity adaptive adjustment embedded control system for electric tractor were integrated (Figure 12).

2.5 Field evaluation test of slip-draft embedded control system during ploughing

The electric tractor with a slip-draft embedded control system by adjusting adaptively battery position was developed for field evaluation test. The test equipment also included double plough, soil compactness tester (model SC900, Spectrum Technologies, Inc. Illinois, U.S).

2.5.1 Adaptability test during ploughing

To study the adaptability of the slip-draft embedded control system by adjusting adaptively battery position at different soil conditions, the ploughing tests with single soil condition and combined soil condition were carried out (Figure 13). And three test conditions with different soil compactness (A: sand, B: gravel, C: clay) were artificially set. In all ploughing tests, electric tractor ploughed at a depth of 20 cm and a driving speed of 0.5 m/s. Among them, the ploughing tests with single soil condition were to set a 50 m long test site for the above three compactness soils respectively. However, the combined soil condition was to combine the above three soils with different compactness in the order of C-B-A-B-C-A-C, and the length of each soil with compactness was 10 m,

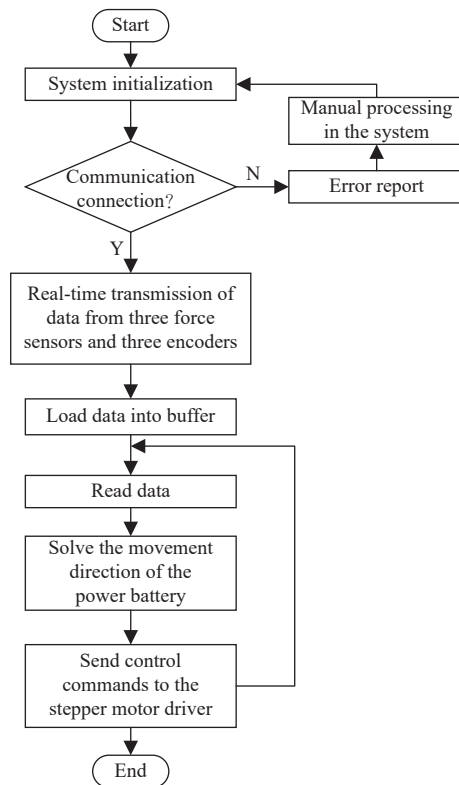


Figure 10 Flow chart of main loop program for developed embedded control system

with a total length of 70 m.

The soil taper coefficient was measured by soil compactness tester, and the measured value was given to the program of slip-draft embedded control system. Then, the ploughing test was carried out with a moldboard plow (model LXT12-20) drove by an electric tractor. And the front wheel load, slip rate and traction efficiency during ploughing were collected by the data acquisition system. The calculation method of traction efficiency^[23] are as follows.

Calculation of the longitudinal wheel offset was expressed in Equation (10).

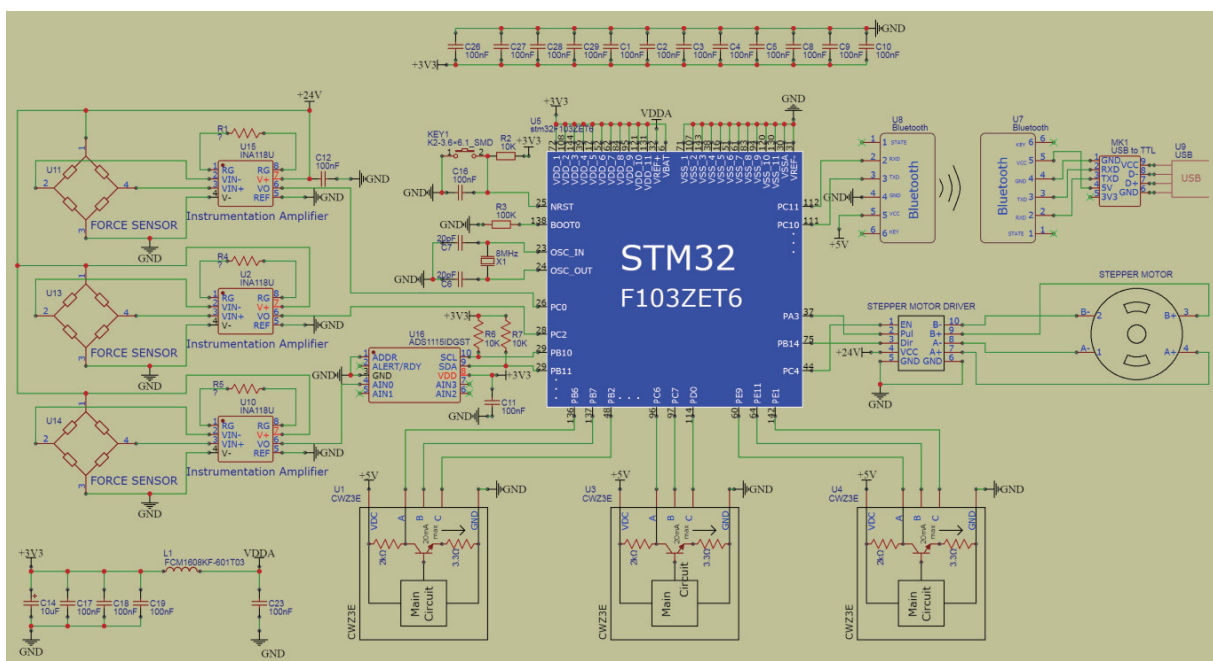


Figure 11 Connecting circuit of each component

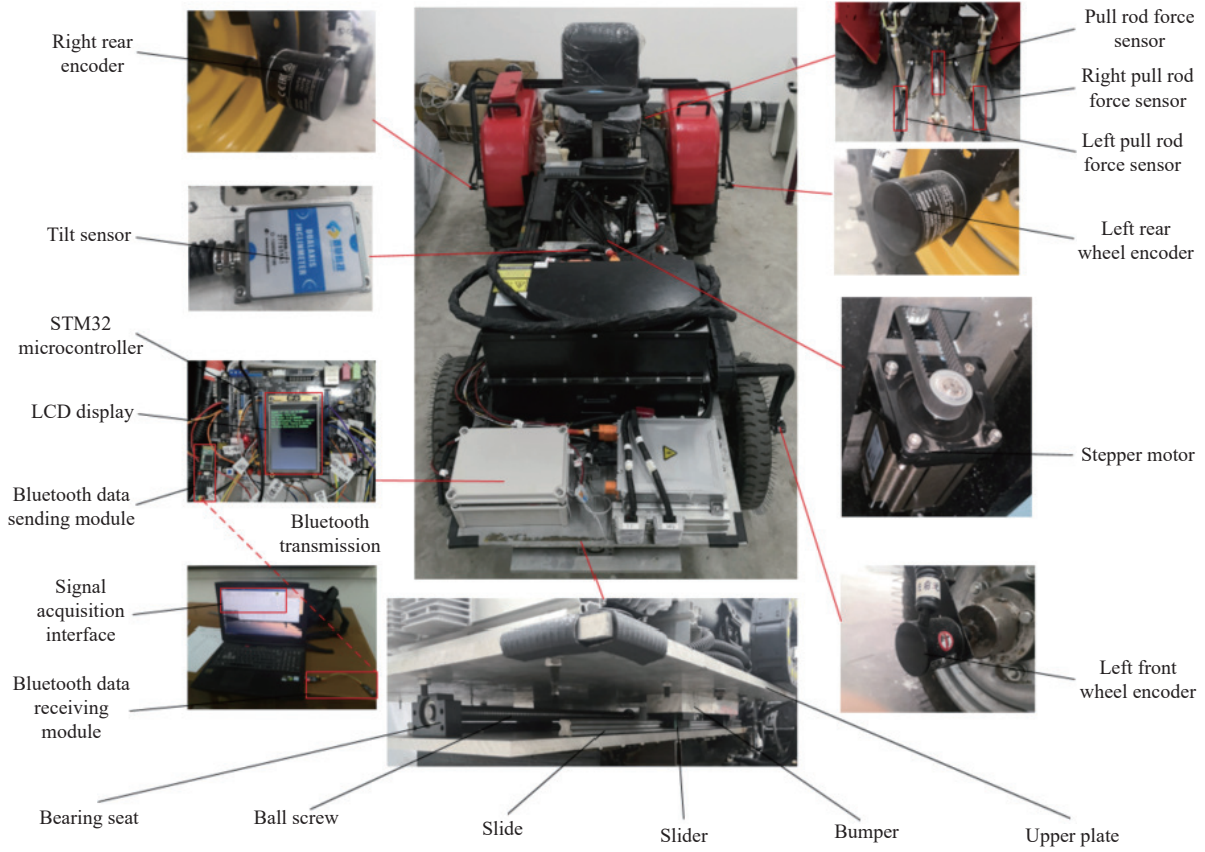


Figure 12 Center of gravity adaptive adjustment embedded control system integration

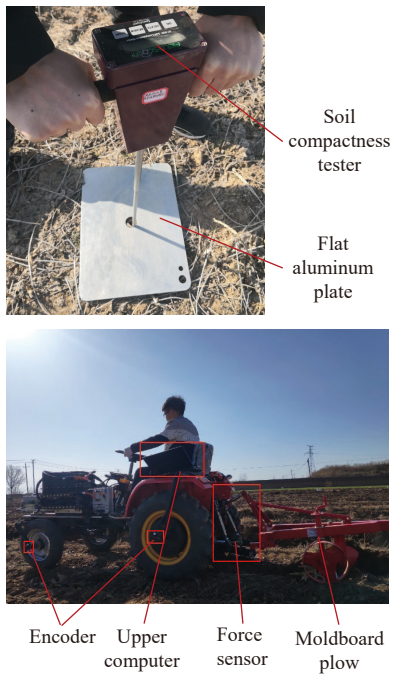


Figure 13 Ploughing test of electric tractor with slip-draft embedded control system

$$\begin{cases} MRR_r = \frac{1}{B_n} + 0.04 + \frac{0.5S}{\sqrt{B_n}} \\ MRR_f = \frac{1}{B_n} + 0.04 \\ B_n = \frac{CIBd_r}{F_{rz}} \left(\frac{1 + 5\frac{\delta}{h_i}}{1 + 3\frac{B}{d_r}} \right) \end{cases} \quad (10)$$

where, MRR_r is the rear wheel movement resistance ratio; MRR_f is the front wheel movement resistance ratio; B_n is the mobility number; CI is the taper index, N/m^2 ; B is the tire section width, m ; d_r is the diameter of rear wheel without load, m ; δ is the tire deformation, m ; h_i is the tire section height, m ; F_{rz} is the vertical load on the rear wheel of the tractor, N .

Calculation of the traction coefficient was expressed in Equation (11).

$$TC = \frac{F_{gx}}{F_{rz}} \quad (11)$$

where, TC is the traction coefficient; F_{gx} is the draft force of electric tractor during ploughing, N .

Calculation of the traction efficiency was expressed in Equation (12).

$$TE = 100 \frac{TC}{TC + MRR_r} (1 - S) \quad (12)$$

where, TE is the traction efficiency, %.

2.5.2 Comparative verification test during ploughing

The electric tractor with slip-draft embedded control system was set to two modes of adaptive adjustment and fixed battery position, and the comparative verification test during ploughing was carried out, under the same operating conditions (Operating condition: clay; Tillage depth: 20 cm; Driving speed: 0.5 m/s; Operation distance: 50 m). The front wheel load, slip rate, traction efficiency and tillage depth during ploughing were recorded by the data acquisition system, to verify the influence of slip-draft embedded control system by adjusting adaptively battery position on traction efficiency and ploughing depth stability of electric tractor. This study used manual methods to measure tillage depth. The ruler was placed flat on the ground as a geodetic datum, and the steel ruler was inserted into the bottom of the plow in the soil to

measure its depth (Figure 14). The 50 sampling points were selected in the direction of plowing operations with steps of 1 m. The three tillage depths along the vertical direction of the tillage direction were measured in each sampling point, and subtracted 10% from each tillage depth. The average value was calculated as the final tillage depth at the current sampling point.

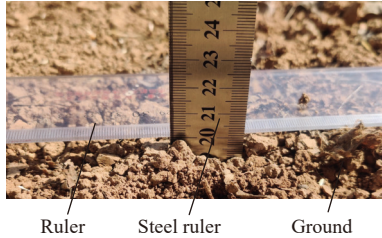


Figure 14 The method of tillage depth measurement test

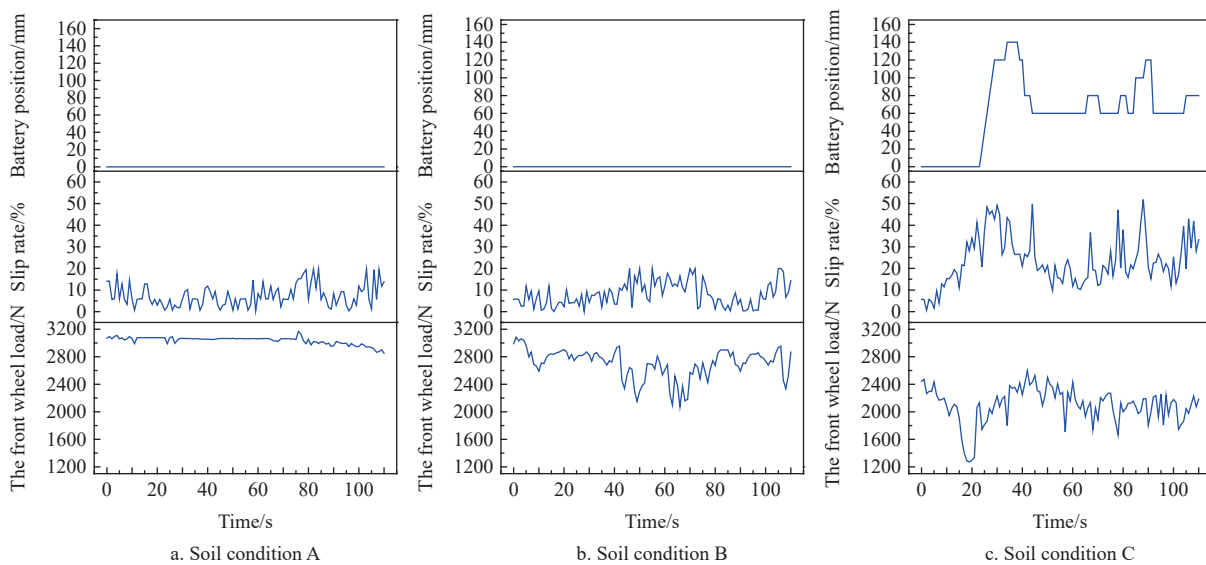


Figure 15 Result of the ploughing tests with single soil condition

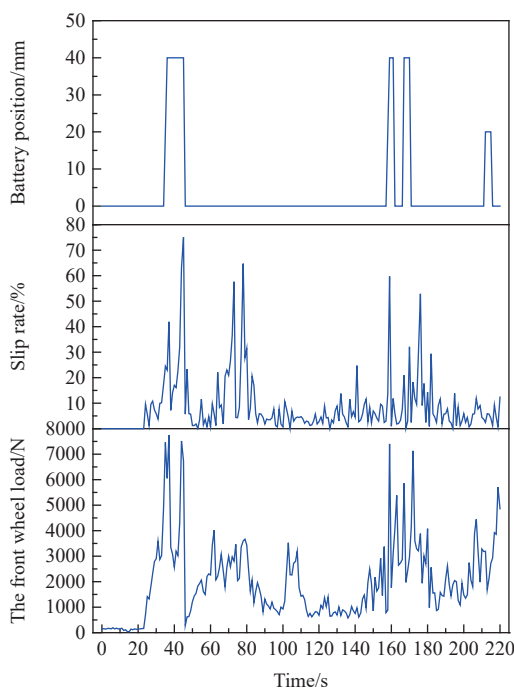


Figure 16 Result of the ploughing test with combined soil condition

3 Results and discussion

3.1 Adaptability test during ploughing

The test results of the ploughing tests with single soil condition and combined soil condition are respectively shown in Figures 15 and 16, which includes the front wheel load, slip rate and battery position. In general, according to the embedded control method for adjusting adaptively battery position shown in Figure 7, the battery position was adjusted only when the front wheel load and slip rate met the judgment conditions.

Specifically, under the soil condition A for ploughing (Figure 15a), the minimum front wheel load was 2851.26 N, the maximum slip rate of the driving wheel was 19.40%, and the battery position was 0.00 mm. Further analysis revealed that the front wheel load was not less than 20% of the vehicle weight, and the maximum slip rate of driving wheel was less than 20% during ploughing in a

sandy soil environment, so the electric tractor did not need to adjust the battery position. And under the soil condition B for ploughing (Figure 15b), the minimum front wheel load was 2151.90 N, the maximum slip rate of the driving wheel was 19.91%, and the battery position was 0.00 mm. When ploughing in a gravel environment, the front wheel load was not less than 20% of the vehicle weight, and the maximum slip rate of driving wheel was less than 20%, so the electric tractor also did not need to adjust the battery position. Significantly, under the soil condition C for ploughing (Figure 15c), the battery position of the electric tractor started to be adaptively adjusted at 24 s. Here, the front wheel load was 1744.70 N, and the slip rate of the driving wheel was 20.60%. Above values met the judgment conditions of the slip-draft embedded control system, but there was a certain degree of delay in the actual adjustment process.

Figure 16 shows the result of the ploughing test with combined soil condition. Among them, when the tractor ploughing environment changed from sand to clay and gravel to clay, the battery position was automatically adjusted, and the adjustment distances in both cases was 40.00 mm. When the control system determined that the front wheel load and slip rate had changed and issued a longitudinal adjustment command for the battery position, the longitudinal adjustment mechanism for the battery position could complete the corresponding adjustment action within 1-2 s. It can meet the adaptive adjustment requirements of the system.

Therefore, the slip-draft embedded control system can adaptively adjust the battery position of electric tractor according to different working conditions, to deal with the changes of different ploughing soil environment.

3.2 Comparative verification test during ploughing

The result of comparative verification test during ploughing is shown in Figure 17, including the front wheel load, slip rate and battery position. The trend of traction efficiency of electric tractors is shown in Figure 18, and the change of tillage depth is shown in Figure 18, and the comparison results of three repeated tests are listed in Table 2.

The result of comparative verification test during ploughing with the slip-draft embedded control system is shown in Figure 17a. From 3 s to 10 s, the front wheel load was less than 20% of the

vehicle weight, and the slip rate of driving wheel exceeded 20%, thus the battery position gradually moved forward to 140 mm. With the forward movement of the battery position, the vertical load of the front wheel showed an upward trend, and the front wheel load reached $0.2 G_T$ at 11 s. Then from 11 to 33 s, the battery position moved backward to reducing the front wheel load while increasing the rear wheel load, because the front wheel load was greater than $0.2 G_T$, and the slip rate was greater than 20%. From 33 to 47 s, the front wheel load and slip rate were within the threshold range, so the battery position remained unchanged. From 47 s to 110 s, the front wheel load of the tractor fluctuated up and down $0.2 G_T$. When the front wheel load was lower than $0.2 G_T$ and the slip rate exceeded 20%, the battery position moved forward and finally remain at a relatively stable position.

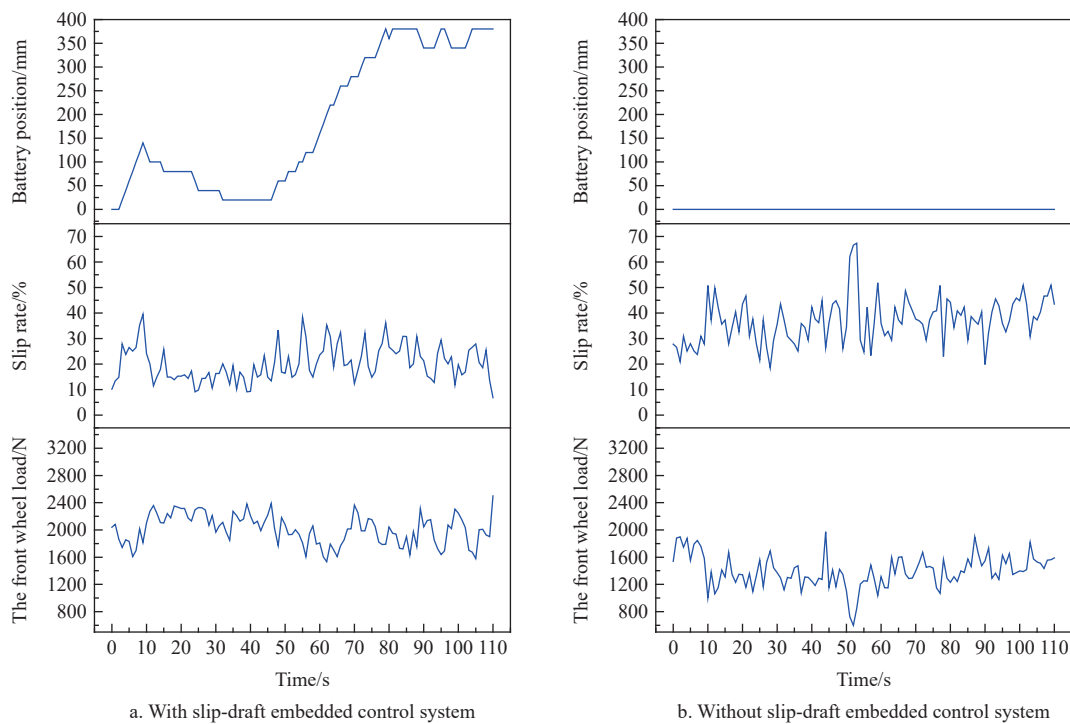


Figure 17 Result of comparative verification test during ploughing

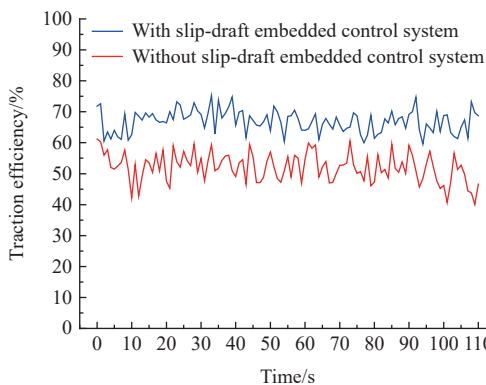


Figure 18 Traction efficiency change of electric tractor during ploughing

The result of comparative verification test during ploughing without the slip-draft embedded control system is shown in Figure 17b. During ploughing of electric tractors, the front wheel load was lower than $0.2 G_T$ and the slip rate of driving wheel was higher than 20%. It was difficult to control the front wheel direction and the tractor was prone to side slip, which seriously affected the

ploughing operation quality and efficiency.

The traction efficiency and the tillage depth stability (Figures 18 and 19) of the electric tractor with the slip-draft embedded control system was greater than that without the slip-draft embedded control system, which proved the feasibility of the slip-draft embedded control system by adaptively adjusting battery position to improve the traction efficiency and the tillage depth stability of electric tractor during ploughing.

Further analysis can be obtained (Table 2), the average traction efficiency, slip rate, front wheel load and relative error of tillage depth of electric tractor using the slip-draft embedded control system by adaptively adjusting battery position were 64.5%, 22.2%, 2045.0 N and 2.0%, respectively. Which were optimized respectively by 15.0%, 29.5%, 19.6% and 80.0%, compared with the electric tractor without the slip-draft embedded control system.

4 Conclusions

(1) A slip-draft embedded control system by adaptively adjusting battery position based on 2WD electric tractor was designed, and the battery of electric tractor was innovatively equivalent to the original counterweight of the fuel tractor. Through

Table 2 Structural performance parameters of electric tractor

Test number	With slip-draft embedded control system				Without slip-draft embedded control system			
	The average slip rate/%	The average front wheel load/N	The average traction efficiency/%	The average tillage depth/cm	The average slip rate/%	The average front wheel load/N	The average traction efficiency/%	The average tillage depth/cm
1	20.5	2063.0	64.6	19.6	37.0	1395.7	53.4	18.0
2	20.4	2004.7	65.4	19.8	30.5	1716.5	58.0	18.3
3	25.8	2067.2	63.6	19.3	33.4	2017.6	56.9	17.8
Average	22.2	2045.0	64.5	19.6	33.6	1709.9	56.1	18.0

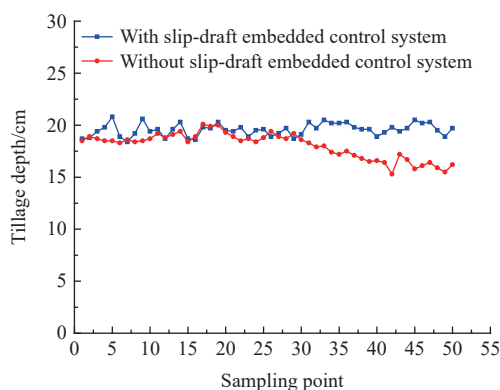


Figure 19 Tillage depth change of electric tractor during ploughing

dynamic analysis of electric tractor during ploughing, the mathematical model of adjusting the center of gravity about draft force and slip rate was established. And the longitudinal for center of gravity of the electric tractor was adjusted by the automatic adjustment of the battery position, to realize the adjustment control of the center of gravity of the electric tractor.

(2) In the adaptability test during ploughing, the electric tractor with the slip-draft embedded control system by adaptively adjusting battery position had strong adaptability. That could automatically adjust the battery position, according to the complex changes of the ploughing operating conditions.

(3) In the comparative verification test during ploughing, the average traction efficiency, slip rate, front wheel load and relative error of tillage depth of electric tractor using the slip-draft embedded control system by adaptively adjusting battery position were 64.5%, 22.2%, 2045.0 N and 2.0%, respectively. Which were optimized respectively by 15.0%, 29.5%, 19.6% and 80.0%, compared with the electric tractor without the slip-draft embedded control system. The verification test showed that the ploughing performance of the electric tractor had been greatly improved, which met the actual requirements of the electric tractor.

Acknowledgements

This research was financially supported by the International cooperation project of Qilu University of Technology (Grant No. QLUTGJHZ2018022). We would like to express our gratitude to all those who have helped us during the writing of this thesis.

[References]

- [1] Moreda G P, Munoz-Garcia M A, Barreiro P. High voltage electrification of tractor and agricultural machinery—A review. *Energy Convers Manage*, 2016; 115: 117–131.
- [2] Wang J, Zhang X M, Zhang B, Hou X N, Song C B, Zhao J Y. Research status and trend of electric agricultural machinery. *Journal of Chinese Agricultural Mechanization*, 2019; 40(10): 35–41. (in Chinese)
- [3] Mousazadeh H, Keyhani A, Javadi A, Mobli H, Abrinia K, Sharifi A. Life-cycle assessment of a solar assist plug-in hybrid electric tractor (SAPHT) in comparison with a conventional tractor. *Energy Convers Manage*, 2011; 52(3): 1700–1710.
- [4] Troncon D, Alberti L. Case of study of the electrification of a tractor: electric motor performance requirements and design. *Energies*, 2020; 13(9): 2197.
- [5] Gupta C, Tewari V K, Kumar A A, Shrivastava P. Automatic tractor slip-draft embedded control system. *Comput. Electron. Agric*, 2019; 165: 104947.
- [6] Sahu R K, Rahman H. A decision support system on matching and field performance prediction of tractor-implement system. *Comput. Electron. Agric*, 2008; 60(1): 76–86.
- [7] Xu S L, Feng C L, Yue Y Y. Type of tractor's ballast and it's application. *Tractor & Farm Transporter*, 2007; 34(4): 100–101. (in Chinese)
- [8] Alonzo K, Byan N, David S, Ranjith U. Field and service applications—An infrastructure-free automated guided vehicle based on computer vision—An effort to make an industrial robot vehicle that can operate without supporting infrastructure. *IEEE Robot Autom Mag.*, 2007; 14(3): 24–34.
- [9] Zhao S X, Liu M N, Xu L Y. Optimization design of electric tractor chassis based on multiple performance objectives. *Transactions of the CSAM*, 2018; 49(Supp): 492–498. (in Chinese)
- [10] Janulevicius A, Pupinis G, Lukstas J, Damanauskas V, Kurkauskas V. Dependencies of the lead of front driving wheels on different tire deformations for a MFWD tractor. *Transport*, 2015; 32(1): 23–31.
- [11] Chen D L, Zuo S L, Liang J L. Effect of counterweight on plowing traction performance of small wheeled tractor. *Tractor & Farm Transporter*, 1990; 17(6): 39–71. (in Chinese)
- [12] Ning P C, Su K, Wang M H, Cui G P, Li K, Cui Y J, Wang W. Design and test of electric tractor with battery position longitudinally adjustable mechanism. *Journal of Agricultural Mechanization Research*, 2022; 44(3): 212–218. (in Chinese)
- [13] Cermak M, Mitas S. Theoretical analysis of the forces and torques acting on a tractor during ploughing. *J Terramechanics*, 2021; 96: 23–27.
- [14] Zhao H C, Zhou S B, Chen W, Miao Z Q, Liu Y H. Modeling and motion control of industrial tractor-trailers vehicles using force compensation. *IEEE/ASME T Mech*, 2021; 26(2): 645–656.
- [15] Yang Q Z, Huang G L, Shi X Y, He M S, Ahmad I, Zhao X Q, et al. Design of a control system for a mini-automatic transplanting machine of plug seeding. *Comput. Electron. Agric.*, 2020; 169: 105226.
- [16] Wu Z B, Xie B, Li Z, Chi R J, Ren Z Y, Du Y F, et al. Modelling and verification of driving torque management for electric tractor: Dual-mode driving intention interpretation with torque demand restriction. *Biosyst Eng*, 2019; 182: 65–83.
- [17] Vidas D. Influence of adjustable front ballast on tractor axles balance. 19th International Scientific Conference Engineering for Rural Development, 2020. Yorgawa, Latvia, 2020; 19: 672–678.
- [18] Pranav P K, Pandey K P, Tewari V K. Digital wheel slipmeter for agricultural 2WD tractors. *Comput. Electron. Agric*, 2010; 73(2): 188–193.
- [19] Liu M N, Zhou Z L, Xu L Y, Zhao J H, Meng T. Electric tractor energy system and management strategy research based on load power spectral density. *Transactions of the CSAM*, 2018; 49(2): 358–366. (in Chinese)
- [20] Xu L Y, Zhao Y R, Zhao X P, Liu M N, Ni Q. Design and test of multifunctional test system for electric tractor. *Transactions of the CSAM*, 2020; 51(1): 355–363. (in Chinese)
- [21] Horton D N L, Crolla D A. The handling behavior of off-road vehicles. *Int. J. of Vehicle Design*, 1984; 5(1-2): 197–218.
- [22] Zhu Z, Gao X, Zhu Y, Pan D Y. Experimental analysis of tractor slip ratio. *Journal of Machine Design*, 2016; 33(8): 62–66. (in Chinese)
- [23] Kumar A A, Tewari V K, Nare B, Chetan C R, Srivastava P, Kumar S P. Embedded digital drive wheel torque indicator for agricultural 2WD tractors. *Comput. Electron. Agric.*, 2017; 139: 91–102.